CrossMark

ORIGINAL ARTICLE

HNF1β drives glutathione (GSH) synthesis underlying intrinsic carboplatin resistance of ovarian clear cell carcinoma (OCCC)

Filipa Lopes-Coelho [1,2] · Sofia Gouveia-Fernandes [1,2] · Luís G Gonçalves [3] ·
Carolina Nunes [1,2] · Inês Faustino [1] · Fernanda Silva [1,2] · Ana Félix [1,4] · Sofia A Pereira [1] ·
Jacinta Serpa [1,2]

Abstract Chemoresistance to platinum-based antineoplastic agents is a consistent feature among ovarian carcinomas; however, whereas high-grade serous carcinoma (OSC) acquires resistance during chemotherapy, ovarian clear cell carcinoma (OCCC) is intrinsically resistant. The main objective of this study was to explore, in vitro and in vivo, if hepatocyte nuclear factor 1β (HNF1β) and glutaminolysis contribute for the resistance of OCCC to carboplatin through the intrinsically increased GSH bioavailability. To disclose the role of HNF1β, experiments were also performed in an OSC cell line, which does not express HNF1β. Metabolic profiles, GSH quantification, HNF1β, and γ-glutamylcysteine ligase catalytic subunit (GCLC) and modifier subunit (GCLM) expression, cell cycle, and death were assessed in ES2 cell line (OCCC) and OVCAR3 cell line (OSC); HNF1β knockdown was performed in ES2 and murine model of subcutaneous and peritoneal OCCC tumors was established to test buthionine sulphoxamine (BSO), as a sensitizer to carboplatin.

Glutaminolysis is activated in ES2 and OVCAR3, though ES2 exclusively synthesizes amino acids and GSH. ES2 cells are more resistant to carboplatin than OVCAR3 and the abrogation of GSH production by BSO sensitizes ES2 to carboplatin. HNF1β regulates the expression of GCLC, but not GCLM, and consequently GSH production in ES2. In vivo, BSO prior to carboplatin reduces dramatically subcutaneous tumor size and GSH levels, as well as peritoneal dissemination. Our study discloses HNF1β as the mediator of intrinsic OCCC chemoresistance and sheds a light to re-explore a cancer adjuvant therapeutic approach using BSO to overcome the lack of efficient therapy in OCCC.

✉ Jacinta Serpa
jacinta.serpa@fcm.unl.pt

1   Centro de Estudos de Doenças Crónicas (CEDOC), NOVA Medical School/Faculdade de Ciências Médicas, Universidade Nova de Lisboa, Campo Mártires da Pátria 130, 1169-056 Lisbon, Portugal

2   Unidade de Investigação em Patobiologia Molecular do Instituto Português de Oncologia de Lisboa Francisco Gentil (IPOLFG), Lisbon, Portugal

3   Instituto de Tecnologia Química e Biológica (ITQB), Oeiras, Portugal

4   Pathology Department, IPOLFG, Lisbon, Portugal

Introduction

Epithelial ovarian cancer (EOC) accounts for 90 % of all ovarian malignancies [1] and is the leading cause of death from gynecological cancer [2, 3]. Risk determinants for EOC are associated with family history, nulliparity, pregnancy, lactation, oral contraceptive use, and tubal ligation [4]. Within EOC, clear cell carcinoma (OCCC) represents a distinct clinical challenge with an unique biology [5]. Despite its low incidence (3–10 % of cases) among EOC, OCCC is highly mortal, when the disease has extraovarian extension [6]. De novo expression of hepatocyte nuclear factor 1β (HNF1β) is a hallmark of OCCC, being essential for cancer cell survival [7, 8]. This transcription factor is also involved in metabolic

Springer

alterations such as glycogen synthesis and cell accumulation, characteristic of OCCC [7, 8].

Chemoresistance is a consistent feature among ovarian carcinoma histological types [3, 9–11]; however, high-grade serous carcinoma (OSC, the most prevalent type) acquires resistance due to cyclic exposure to drugs and OCCC is intrinsically resistant to chemotherapy. Hence, in tumor recurrence and when diagnosed at an advanced stage, OCCC is an incurable disease [12, 13].

Carboplatin is a second-generation platinum-containing antineoplastic drug used in conventional ovarian cancer therapy. This drug acts by two main mechanisms: the establishment of covalent bounds with DNA and proteins and the generation of reactive oxygen species (ROS) [14–17]. ROS and carboplatin are able to react with sulfur-containing molecules, as glutathione (GSH) and other thiols [18, 19]. Glutathione (GSH) is the main ROS cell scavenger, acting on detoxification and cell protection. The key enzyme in GSH modulation is γ-glutamylcysteine ligase (GCL), composed by a catalytic subunit (GCLC) whose activity is modulated by a second subunit (GCLM) [20, 21]. Despite the fact that DNA is considered the main target of platinum drugs, these drugs react with cytosolic thiol pool before reaching the nucleus, contributing also for drug resistance [22]. As claimed in some studies, molecular alterations in GSH and other thiols in a variety of tumors can lead to an increased cell survival and tumor drug resistance [18, 23–25].

Tumor metabolism is considered a hallmark in cancer [26, 27] and despite its role in carcinogenesis, it is not completely known, the relevance of metabolic adaptation in cancer progression is inescapable. As mentioned above, HNF1β is responsible for glycogen accumulation in OCCC, showing that glucose might not be the main carbon and energy source for these cells. Amino acids are relevant sources for biomass production and energy sustenance, and glutamine can play a leading role in metabolism due to its anaplerotic character as a carbon and nitrogen source for the synthesis of nitrogen and carbon skeletons. Hence, glutamine is a very good candidate to overlap the metabolic adaptations of OCCC. Importantly, glutamine is also a crucial precursor of amino acids for GSH biosynthesis [28, 29].

The main objective of this study was to explore if HNF1β and glutaminolysis contribute for the GSH bioavailability, which may be responsible for the intrinsic resistance of OCCC to platinum-based chemotherapy through its increase (Fig. 1). A cell line which does not express HNF1β, the OSC, was also used in order to unveil its role.

Experimental procedures

Cell culture Cell lines from OCCC (ES2; CRL-1978) and OSC (OVCAR-3; HTB-161) were obtained from American Type Culture Collection (ATCC). Cells were maintained at 37 °C in a humidified 5 % CO$_2$ atmosphere. Cells were cultured in DMEM 1× (41965-039, Invitrogen™, Life Technologies) containing 4.5 g/L of D-glucose and 0.58 g/L of L-glutamine or DMEM without both D-glucose and L-glutamine (F 0450, Biochrom) supplemented with 1 % FBS (S 0615, Invitrogen), 1 % antibiotic-antimycotic (AA) (15240062, Invitrogen) and exposed either to 4 mM L-glutamine (250330-81, Invitrogen™, Life Technologies) and/or 0.420 mM L-cysteine (168149, Sigma-Aldrich).

Prior to any experiment, cells were synchronized under starvation (culture medium without FBS), overnight at 37 °C and 5 % CO$_2$.

Nuclear magnetic resonance (NMR) assay Cells (~5×10^7) were cultured in 125-cm^2 tissue culture flasks and exposed to 8 mM ^{13}C-[U]-L-glutamine (605166, Sigma-Aldrich) in DMEM without both D-glucose and L-glutamine supplemented with 1 % FBS and 1 % AA for 48 h. Supernatants were collected and stored at −80 °C.

High-performance liquid chromatography (HPLC) Cells (6.5×10^6) were cultured in 75-cm^2 tissue culture flasks in control conditions and exposed to either 4 mM L-glutamine and/or 0.420 mM L-cysteine for 16 h. The same experiment was developed in the presence of carboplatin (10 ng/mL). The supernatants were stored at −80 °C.

Cell cycle analysis Cells (2.5×10^4 cells/well) were seeded in 24-well plates and cultured in control condition and exposed to 4 mM L-glutamine and/or 0.420 mM L-cysteine and collected at 6, 12, 24, 32, 48, and 60 h after stimulation.

Cell death analysis Cells (2.5×10^4 cells/well) were seeded in 24-well plates and maintained in control conditions and were treated with different combinations of carboplatin (25 μg/mL) and H$_2$O$_2$ (98 μM) (positive control) for 16 h. Whenever applied, cells were either previously exposed to buthionine sulphoxamine (BSO) (20 mM) for 48 h.

Chromatin immunoprecipitation (ChIP) Cells (5×10^7) were cultured in 125-cm^2 tissue culture flasks in control conditions and exposed to 4 mM L-glutamine and 0.420 mM L-cysteine for 48 h.

Nuclear magnetic resonance Cell extracts were performed with methanol and chloroform in order to separate organic and aqueous phases. After cold methanol mixture (4 mL methanol/ 1 g weight pellet), 1 volume of water was added, mixed, and incubated for 5 min on ice. Chloroform (1 volume) was added to the sample and mixed. Then, 1 volume of water was added and samples were incubated for 10 min on ice, following centrifugation at 4000 rpm for 15 min at 4 °C. Aqueous (upper) and organic (lower) phases were collected. Lyophilization of the
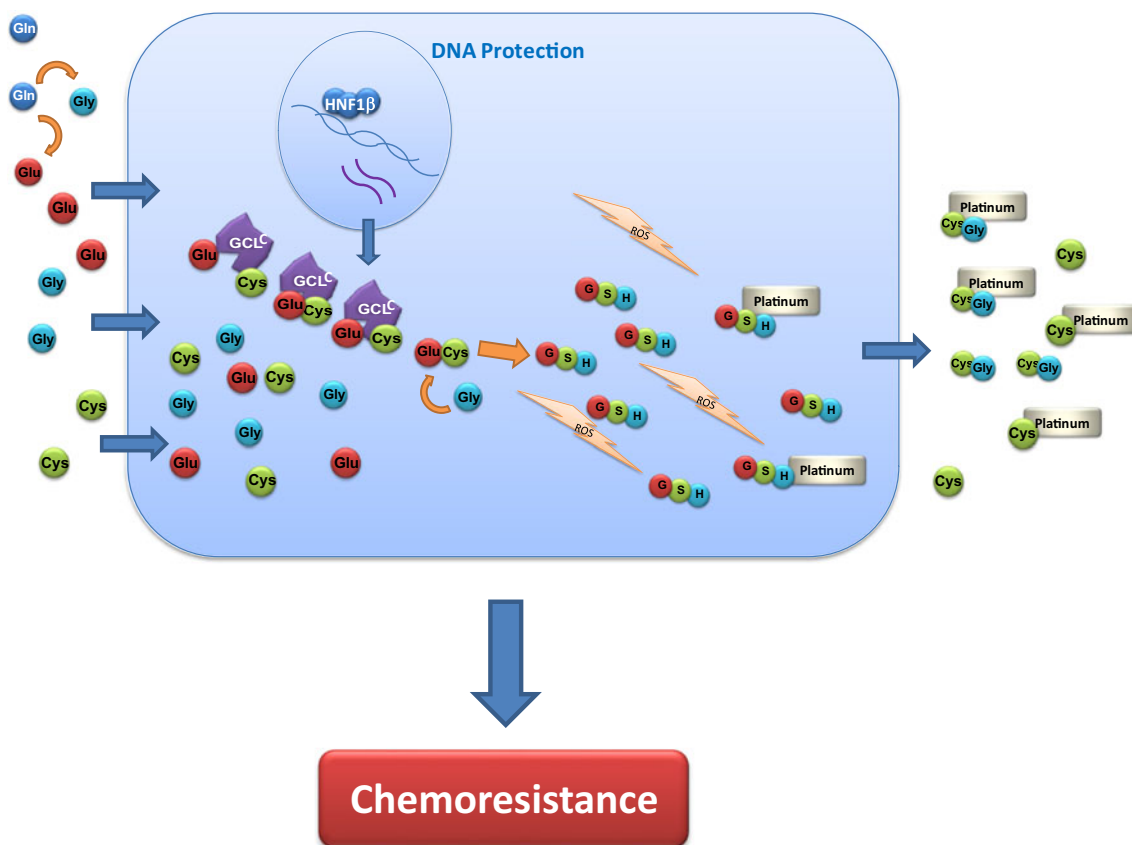
Fig. 1 Scheme of molecular mechanism underlying thiol mediated chemoresistance in OCCC. Glutaminolysis is essential for GSH synthesis, as L-glutamine (Gln) it is the direct source of L-glutamate (Glu) and L-glycine (Gly) that compose, together with L-cysteine (Cys), the scavenger molecule, glutathione (GSH). HNF1β, the defining gene of OCCC, regulates the expression of γ-glutamylcysteine ligase (GCL), which catalyzes the limiting step of GSH synthesis, promoting high levels of GSH. Besides the antioxidant role of GSH, thiols (GSH, CYS-GLY, Cys) can confiscate platinum molecules in and outside the cell, avoiding it to reach cell components and the formation of protein and DNA adducts

aqueous phase was performed using Speed Vac Plus Scllon and then dissolved in deuterated water (D$_2$O) and 4 % (*v/v*) sodium azide (NaN$_3$)/4,4-dimethyl-4-silapentane-1-sulfonic acid (DSS) solution (1:10). Culture supernatants were also diluted in this solution at 1:10 ratio. The 1H-NMR (noesypr1d) and ^{13}C,^{1}H-HSQC 2D spectra were obtained at 25 °C in Ultrashied™ 800 Plus (Bruker) operating at 800.33 MHz, equipped with a TXI-Z H C/N/-D (5 mm) probe. Proton decoupled ^{13}C-NMR spectra were acquired in a Bruker AVANCE III 500 (Bruker) at 125.77 MHz, using a 5-mm ^{13}C selective probe head at 25 °C. The chemical shifts in aqueous sample were referred to (trimethylsilyl)propanesulfonic acid, while the samples in chloroform-d were referred to the solvent signal designated at 77.0 ppm. Topspin 2.1 on avance 800 (Bruker) was used for acquisition and spectra analysis; compound identification was performed by resorting to the Human Metabolome database (HMDB) (http://www.hmdb.ca/) and Chemomx NMR suite 7.6.

HNF1β knockdown in ES2 by shRNA transfection
HNF1β knockdown was generated in ES2 cell line. For this purpose, ES2 cells were transfected with HNF1β shRNA plasmid (KH00020N, Quiagen) and Control shRNA plasmid (SC-108060, Santa Cruz). Transfection was carried out with Lipofectamine 2000 (11668, Invitrogen), according to the manufacturer's protocol. Transfected cells were selected with geneticin (G418) (10131-027, Gibco) and puromycine (A11138-03, Invitrogen), respectively, for HNF1β shRNA plasmid and control shRNA plasmid.

In vivo studies the animal handling and experimental procedures were performed under the rules of Federation for Laboratory Animal Science Associations (FELASA), accomplishing the 3Rs through evidence-based guidelines. Female BALB-c/SCID mice (6 weeks, 20 g weight) maintained in a pathogen-free barrier room in the Animal Care Facility at the *Instituto Gulbenkian de Ciência* were used to develop subcutaneous (SC) and intraperitoneal (IP) tumors by ES2 cells inoculation (3×10^5 cells/mice). Two weeks post-inoculation, when SC tumor was detected by touch, mice were treated once a week as follows: control (0.9 % NaCl), BSO (1 mM/kg), carboplatin (100 mg/kg), and BSO (1 mM/kg) plus carboplatin (100 mg/kg). BSO was diluted in 0.9 % NaCl solution and administrated 24 h before carboplatin [30, 31]. When SC tumor volume in BSO plus carboplatin group

became undetectable by touch, all mice were sacrificed and necropsy was performed.

High-performance liquid chromatography Cell extracts were performed by lysing cells with 200 µL of Triton X-100 (0.01 %) in PBS 1× (*v/v*) followed by centrifugation at 2000 g for 2 min, 4 °C. The lysis supernatant was centrifuged in an Amicon® Ultra 10K device (Millipore) at 3800 g for 20 min, 4 °C. Equal mass of tumor (0.3 mg) was dissociated in PBS 1× by sonication (1 cycle, 10 s, 50 % amplitude) followed by centrifugation in an Amicon® Ultra 10 K device (Millipore) as in cell lysis. The aminothiols in cell extracts, culture media (supernatants), crude culture medium, and tumor extracts (100 µL) were reduced with tris(2-carboxyethyl)phosphine (TCEP); the proteins were precipitated with trichloroacetic acid; and reduced thiols were derivatized with ammonium 7-fluoro-2,1,3-benzoxadiazole-4-sulfonate (SBD-F), according to Nolin et al. [50]. Samples were analyzed by HPLC system (Shimadzu) with a RF 10AXL fluorescence detector, operating at 385 nm (λ exCitation) and 515 nm (λ emission). The aminothiols HCY, CYS, CysGly, and GSH were separated on a *LiChrospher* 100 RP-18 (250×4 mm, 5 µm; Merck), with a mobile phase consisting on a mixture of 0.1 M acetate buffer (pH 4.5, adjusted with acetic acid): methanol (99:1 *v/v*) at a flow rate of 0.8 mL/min at 29 ° C. The run time was 20 min.

Fluorescence-activated cell sorting (FACS) For cell cycle analysis, cells were collected and fixed in 70 % ethanol (100983, Merck) and stored at 4 °C. Cells were centrifuged at 1500 rpm for 5 min and then stained with 100 µL propidium iodide (PI) solution (50 µg/mL PI, 1001498536; Sigma), 0.1 mg/mL RNase (RN-001, Citogene), 0.05 % Triton X-100) and incubated at 37 °C for 40 min. PBS 1× was added after incubation and cells were centrifuged at 1500 rpm for 10 min at 4 °C. The supernatant was discarded and cells were resuspended in 200 µL of 0.2 % (*w/v*) BSA (bovine serum albumin) (A9647, Sigma) in PBS 1× and analyzed by FACS (FACScalibur–Becton Dickinson. Data were analyzed using FlowJo (http://www.flowjo.com/) software.

Cell death quantification Cells were harvested by centrifugation at 1200 rpm for 2 min, cells were incubated with 1 µL annexin V-Alexa Fluor® 488 (640906, BioLegend) and 1 µL PI (50 µg/mL) in 100 µL annexin V binding buffer 1× (10 mM HEPES (pH 7.4), 0.14 M sodium chloride (NaCl), 2.5 mM calcium chloride (CaCl$_2$)) and incubated at room temperature and in the dark for 15 min. After incubation, samples were rinsed with 0.2 % (*w/v*) BSA (A9647, Sigma) in PBS 1× and centrifuged at 1200 rpm for 2 min. Cells were suspended in 200 µL of annexin V binding buffer 1×. Acquisition was performed in a FACScalibur (Becton Dickinson). Data were analyzed with FlowJo (http://www.flowjo.com/) software.

Immunofluorescence Cells were grown on glass slides with a 0.2 % gelatin coating, in control conditions and 4 mM L-glutamine plus 0.420 mM L-cysteine, until 80 % of confluence and then fixed in 2 % paraformaldehyde for 15 min at 4 °C. Blocking was performed with 0.2 % (*w/v*) BSA in PBS 1× for 1 h at room temperature and incubated with primary antibody overnight (diluted in 0.2 % (*w/v*) BSA in PBS 1×, 1:100). The primary antibody was an anti-human HNF1β (HPA002083, Sigma-Aldrich), anti-human GCLC (DR1045, Millipore), and anti-human GCLM (PA5-29384, Thermo Scientific). Samples were incubated with secondary antibody for 2 h at room temperature. Secondary antibody used was Alexa Fluor® 488 anti-rabbit (A-11078, Invitrogen™, Life Technologies) and Alexa Fluor® 488 anti-mouse (A-11001, Invitrogen™, Life Technologies). The slides were mounted in VECTASHIELD media with DAPI (4′-6-diamidino-2-phenylindole) (Vector Labs) and examined by standard fluorescence microscopy using an Axio Imager.Z1 microscope (Zeiss). Images were acquired and processed with CytoVision® software.

Chromatin immunoprecipitation In order to cross-link DNA and proteins, 37 % formaldehyde was added to the cells at a final concentration of 1 % (*v/v*) and incubated for 10 min at room temperature. After that, 125 mM glycine pH 9 was added, followed by an incubation of 5 min at room temperature. Then, cells were scraped in PBS 1×, centrifuged at 1200 rpm for 2 min and 500 µL of ChIP lysis buffer (kchonedIP-060, Diagenode) were added. Cells in ChIP lysis buffer were stored at −80 °C until sonication.

Lysates were thawed on ice and then sonicated (10 cycles of 30 s, 50 % amplitude). Chromatin fragmentation (between 500–1000 bp) was confirmed using 2 µL of sheared chromatin in a 1.2 % (*w/v*) agarose gel electrophoresis (in 1× TBE buffer (diluted from 10× TBE, EC-860, National diagnostics)) stained with 0.05 % (*v/v*) ethidium bromide). ChIP was performed using OneDay ChIP kit (kch-onedIP-060, Diagenode) according to the manufacturer's protocol. Anti-HNF1β antibody and a rabbit non-immune IgG (negative control) (kch-onedIP-060, Diagenode) were used. The amplification and analysis of immunoprecipitated DNA was performed through RQ-PCR, in an ABI PRISM 7900HT Sequence Detection System (Applied Biosystems) using specific primers (pHNF1β-binding site GCLC FW CTATCATGTACTCACTCATTTAGC:, pHNF1β-binding site GCLC REV: GTGTTGACAGAGCAATGACCTG and pHNF1β-binding site GCLM FW: CTTGAGTTCAGAAGATAGTTATATCGG, pHNF1β-binding site GCLM REV: GTGAAAGAGCTACCCACAAGCAC) designed for a HNF1β binding site at catalytic (GCLC) and modifier subunit (GCLM) of GCL gene promoter region based on TFSearch database analysis. Data were analyzed in SDS 2.4.1 software (Applied Biosystems) and relative occupancy of the immunoprecipitated factor at specific *loci* was calculated using the following equation:

2^(CtNegCtl−CtTarget), where CtNegCtl and CtTarget are the average threshold cycles of PCR triplicates on DNA samples from negative control ChIP (rabbit non-immune IgG) and HNF1β targeted ChIP, respectively.

Statistical analysis Data were analyzed using two-way ANOVA and Student's t tests with GraphPad Prism 5 software. Statistically significant changes were determined at the p value of <0.05.

Results

Glutaminolysis is active in ES2 and OVCAR3 cell lines; ES2 produces exclusively amino acids and GSH from glutamine

In order to define L-glutamine metabolic profile in OCCC and OSC, cell lines were cultured in medium supplemented with ^{13}C-labeled L-glutamine (^{13}C-[U]-L-glutamine), in the absence of D-glucose, and further analyzed by NMR (Fig. 1a, b).

The results obtained showed the presence of ^{13}C labeled glutaminolysis resulting products, confirming its activation in both cell lines (Fig. 2a). Although each cell line shows a different metabolic profile, in ES2, glutaminolysis results mainly in the synthesis of amino acids and GSH and in OVCAR3, besides amino acids and GSH, malate and glycerophosphocholine are also detected (Fig. 2a). Malate is an intermediate of the TCA cycle and glycerophosphocholine is a metabolite involved in the phosphatidylcholine metabolism. In the analysis of supernatants from both cell lines, the main detected compounds were amino acids in different patterns: in ES2, L-asparagine and ornithine are found, while in OVCAR3, L-threonine and aromatic amino acids (L-phenyalanine and L-tyrosine) are detected (Fig. 2a).

The supplementation of cell growth medium with L-glutamine and L-glutamine plus L-cysteine, in replacement of D-glucose, has shown to impact cell proliferation in comparison to control condition (absence of both amino acids and D-glucose), by increasing cell division, here inferred by the increased number of cells undergoing phases S and G2–M. Cell cycle analysis has revealed different cell proliferation rates between the two cell lines, OVCAR3 being, overall, more proliferative than ES2 (Fig. 2b).

Total aminothiol levels are altered by carboplatin exposure in ES2 and OVCAR3; overall ES2 express higher levels of GSH than OVCAR3. Ratio GSH/CYS-GLY indicates a continuous GSH production in ES2

HPLC analysis allowed the intra- and extracellular quantification of total contents of L-cysteine (CYS), homocysteine (HCYS), L-cysteine-L-glycine (CYS-GLY), and GSH (Figs. 3 and 4). Overall, the results displayed increased levels of total aminothiol content in L-glutamine plus L-cysteine condition, in comparison to control, predominantly inside the cells, being significantly increased in ES2 (OCCC) compared to OVCAR3 (OSC) (Fig. 3).

In particular, L-cysteine consumption, HCYS, CYS-GLY, and GSH levels were higher in ES2 than in OVCAR3, being more evident in cells cultured with L-glutamine plus L-cysteine (Fig. 3 and 4). GSH levels were significantly increased in ES2 cell line (2.75- and 2-fold for control and L-glutamine plus L-cysteine conditions, respectively) comparing to OVCAR3 (Fig. 3d).

In the presence of carboplatin, higher levels of extracellular (supernatants) CYS-GLY were detected in ES2 (in all conditions) than in OVCAR3 cell line (Fig. 4c). Regarding intracellular CYS-GLY levels, a decreased expression was observed in ES2 and OVCAR3 both in control and L-glutamine plus L-cysteine conditions due to carboplatin (Fig. 3c).

GSH intracellular levels in ES2 and OVCAR3 increased by carboplatin exposure, except in L-glutamine plus L-cysteine condition, in which they decrease, although these were still high in ES2, and remain unaltered in OVCAR3. However, GSH levels were always higher in ES2 than in OVCAR3 (Fig. 3d). Considering extracellular GSH levels, in ES2, these were almost the same with and without carboplatin exposure, in contrast to OVCAR3, where carboplatin increased significantly GSH levels (Fig. 4d).

Inhibition of GSH synthesis by BSO sensitizes ES2 cells for carboplatin-induced cell death

Buthionine sulfoxamine (BSO) is an inhibitor of γ-glutamylcysteine ligase (GCL), a key enzyme in GSH biosynthesis that catalyzes the formation of γ-glutamylcysteine from L-glutamine and L-cysteine [32]. In order to investigate GSH putative direct involvement in OCCC chemoresistance, cell death induced by carboplatin plus BSO was assessed in both cell lines. The decrease in GSH levels upon BSO exposure was confirmed in both cell lines at 24 and 48 h after incubation (supplementary Fig. 1). The results displayed a consistent increase in cell death of OVCAR3, in comparison to ES2, either by carboplatin or with H_2O_2 (positive control), independent of BSO (Fig. 5b). In fact, in OVCAR3, BSO affected cell viability by itself as seen in microscopic images showing generalized detachment of OVCAR3 cells treated with BSO for 48 h, whereas ES2 cells continued adherent (Fig. 5a). For ES2, cell viability was shown to be compromised only

A

Supernatants — ES2 / OVCAR3

Cell extracts — ES2 / OVCAR3

B
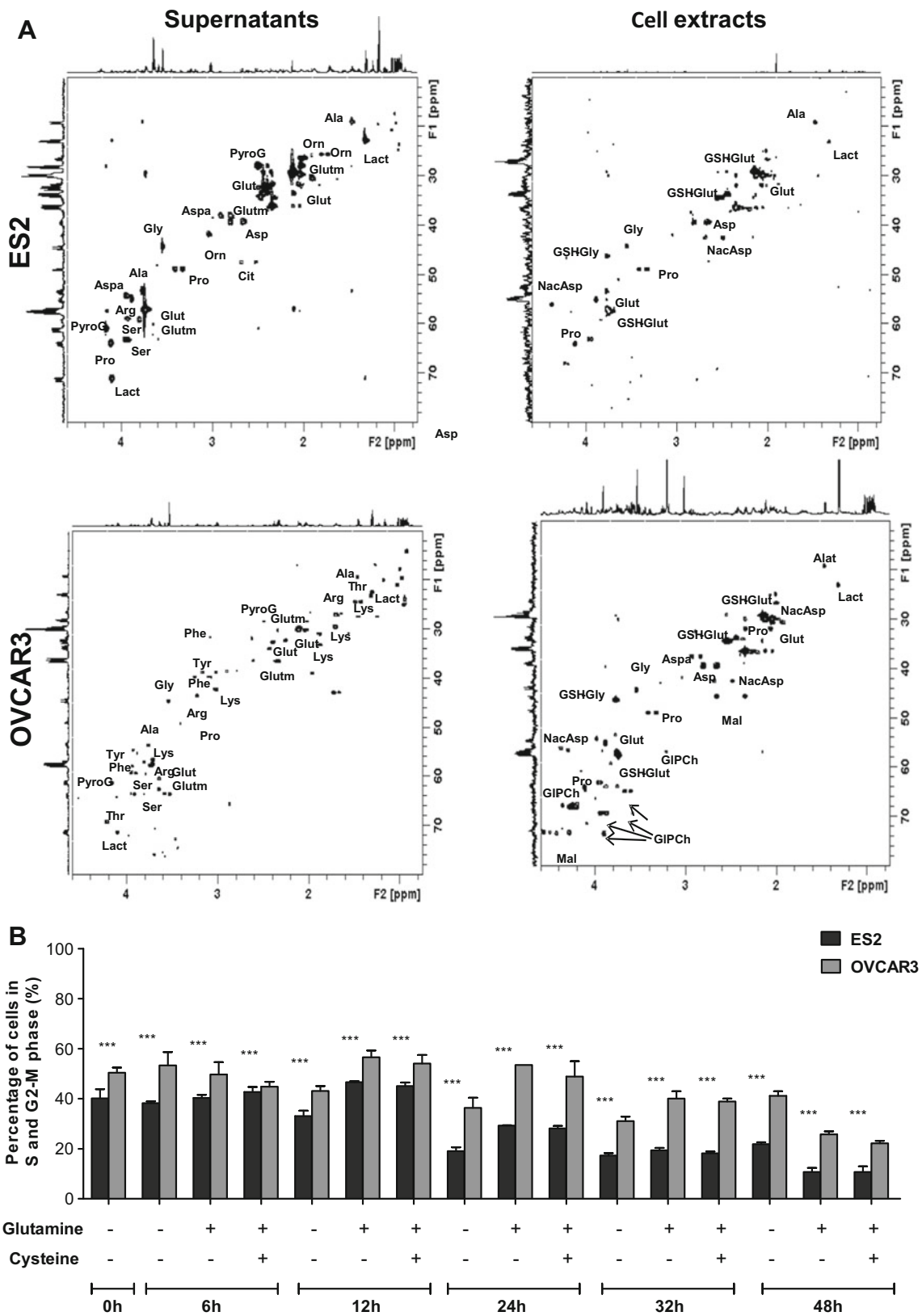
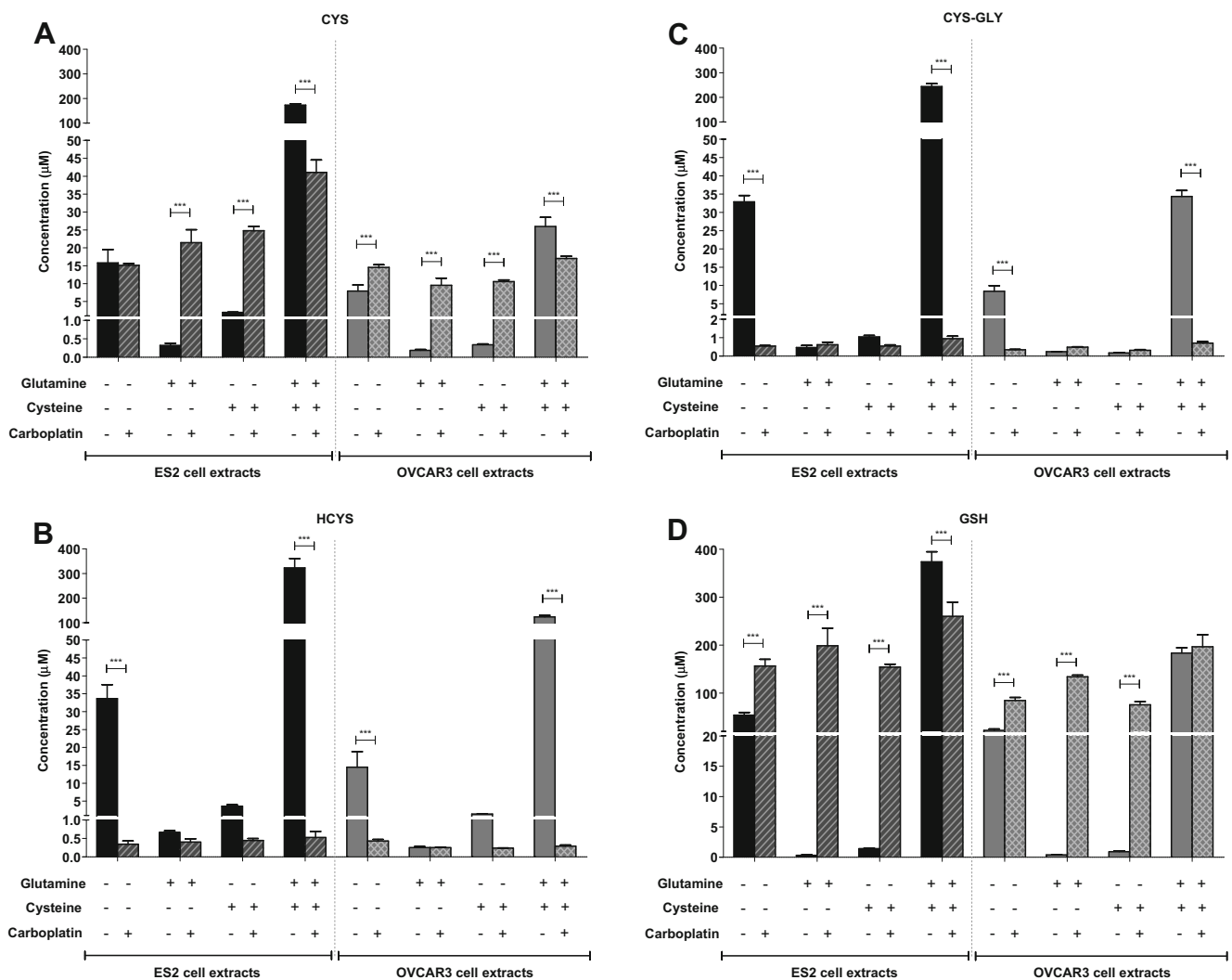when cells previously treated with BSO were exposed to carboplatin and/or H_2O_2, being reached the higher percentage of cell death upon the combination of BSO, carboplatin, and H_2O_2 (Fig. 5b).

◀ **Fig. 2** Glutaminolysis is active in ES2 and OVCAR3 cell lines; ES2 produces exclusively amino acids and GSH from glutamine. **a** ^{13}C-^{1}H-HSQC NMR spectra of supernatants and lysates from cells cultured with ^{13}C-[U]-L-glutamine for 48 h. The ^{13}C labeled compounds identified were *Ala*, alanine; *Aspa*, asparagine; *Asp*, aspartate; *GlPCh*, glycerophosphocholine; *Glut*, glutamate; *Glutm*, glutamine; *GSH-Glu*, glutamate moiety of glutathione; *GSH-Gly*, glycine moiety of glutathione; *Gly*, glycine; *Lact*, lactate; *Lys*, lysine; *Mal*, malate; *NacAsp*, N-acetyl-aspartate; *Orn*, ornithine; *Pro*, proline; *Phe*, phenylalanine; *PyroG*, pyroglutamate; *Ser*, serine; *Thr*, threonine; and *Tyr*, tyrosine. **b** Cell cycle analysis of ES2 and OVCAR3, focusing the sum of the percentage of cells in S and G2–M phases. Experimental conditions included exposures of 6, 12, 24, 32, and 48 h, after starvation, with medium supplemented with 1 % FBS, in absence of D-glucose without L-glutamine and L-cysteine (control), with L-glutamine and with L-glutamine plus L-cysteine. *Error bars* represent standard deviation; statistical significance *$p<0.05$, **$p<0.01$, ***$p<0.001$

## HNF1β regulates γ-glutamylcysteine ligase catalytic subunit (GCLC) not modifier subunit (GCLM) expression and GSH production in ES2. HNF1β downregulation sensitizes cells to carboplatin

As mentioned before, HNF1β expression is a distinctive mark of OCCC. By immunofluorescence, ES2 were positive for HNF1β expression whereas OVCAR3 were negative (Fig. 6a).

Given the relevance of HNF1β in OCCC in cell survival, we decided to verify its role in GSH production through the regulation of GCL gene expression, which has HNF1β binding sites in its 5′ promoter region. As seen by NMR, glutaminolysis provides L-glutamate and L-glycine, two of

Fig. 3 Aminothiol levels are altered by carboplatin exposure in ES2 and OVCAR3; overall ES2 express higher levels of GSH than OVCAR3. Intracellular aminothiol levels were quantified by HPLC both in ES2 (OCCC) and OVCAR3 (OSC). CYS (**a**), HCYS (**b**), CYS-GLY (**c**), and GSH (**d**) quantification in cells cultured for 16 h in medium supplemented with 1 % FBS, with or without carboplatin exposure, in the absence of D-glucose without L-glutamine and L-cysteine (control), with L-glutamine, with L-cysteine, and with L-glutamine plus L-cysteine. *CYS* L-cysteine, *GSH* glutathione, *CYS-GLY* L-cysteine-L-glycine. Results are presented after subtraction of the values obtained for each sample to the values detected in crude media. *Error bars* represent standard deviation; statistical significance *$p<0.05$, **$p<0.01$, ***$p<0.001$
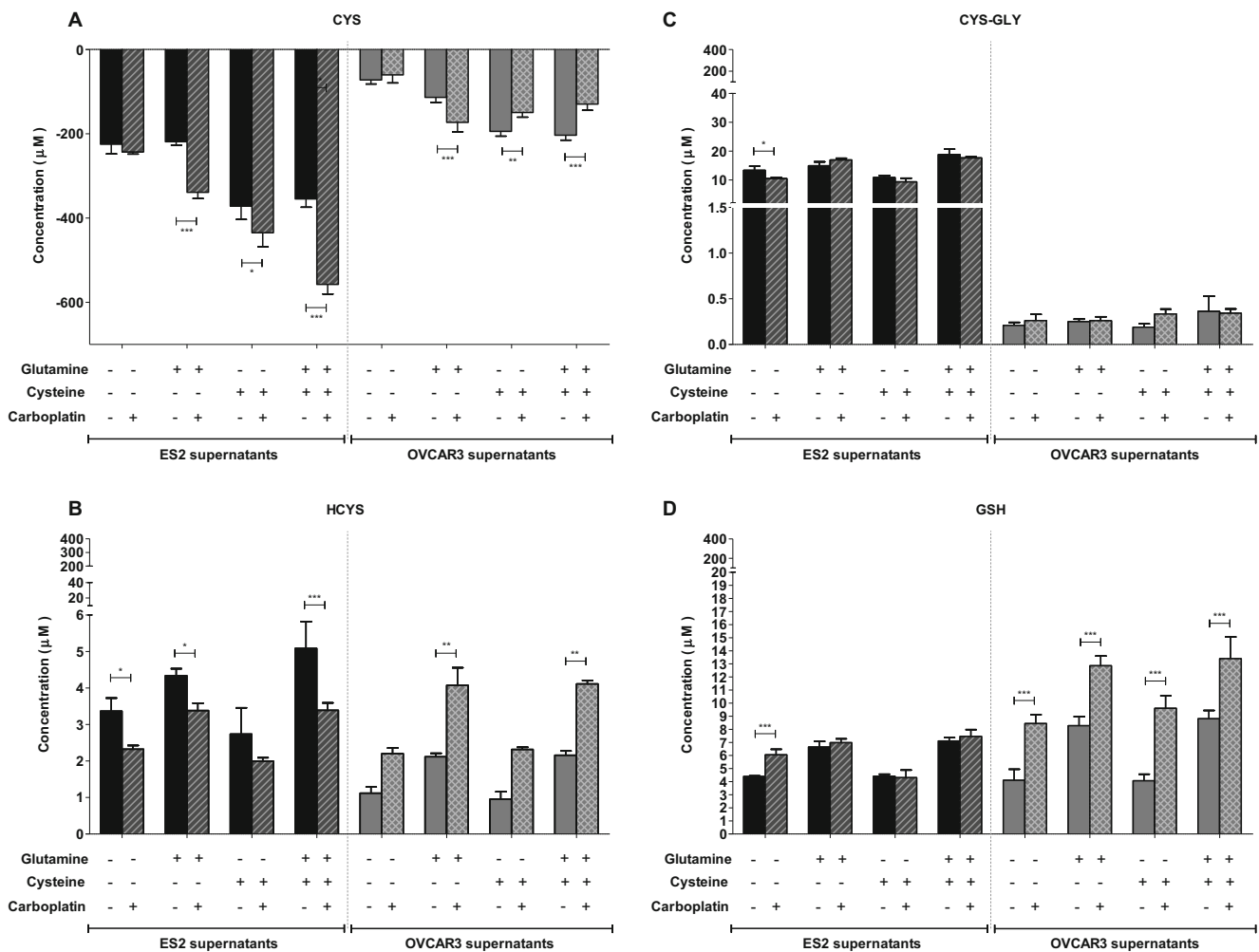
Fig. 4 Carboplatin increases CYS uptake in ES2, contributing for GSH production and increases GSH extracellular levels in OVCAR3 due to cell death; overall CYS-GLY extracellular levels are higher in ES2 than OVCAR3. Extracellular aminothiol levels were quantified by HPLC both in ES2 (OCCC) and OVCAR3 (OSC). CYS (**a**), HCYS (**b**), CYS-GLY (**c**), and GSH (**d**) quantification in cells cultured for 16 h in medium supplemented with 1 % FBS, with or without carboplatin exposure, in the absence of D-glucose without L-glutamine and L-cysteine (control), with L-glutamine, with L-cysteine and with L-glutamine plus L-cysteine. *CYS* L-cysteine, *GSH* glutathione, *CYS-GLY* L-cysteine-L-glycine. Results are presented after subtraction of the values obtained for each sample to the values detected in crude media. *Error bars* represent standard deviation; statistical significance *$p<0.05$, **$p<0.01$, ***$p<0.001$

the three amino acid components of GSH; hence, cells were cultured in L-glutamine plus L-cysteine medium, since L-cysteine is the third amino acid present in GSH molecule. By ChIP assay, we observed a statistically significant increase in the relative occupancy of GCLC promoter by HNF1β but not in GCLM promoter when ES2 cells are cultured with GSH precursor-enriched medium. In OVCAR3 cells, no alterations were observed (Fig. 6b).

Accordingly, by immunofluorescence, it was observed that GCLC expression is higher in ES2 cultured in L-glutamine plus L-cysteine medium. The same was not true for OVCAR3, which express low GCL levels (Fig. 6c). Concerning the expression of GCLM, the levels remained unchanged in both cell lines independent of the exposure

to L-glutamine and L-cysteine. However, OVCAR3 has higher GCLM basal levels than ES2 (Fig. 6c).

The confirmation that HNF1β regulates GCLC in OCCC was made by knocking down HNF1β expression, using shRNA (Fig. 7a). ES2 cells HNF1β knockdown

Fig. 5 Inhibition of GSH synthesis by BSO sensitizes ES2 cells for ▶ carboplatin induced cell death. **a** Phase microscopy of ES2 and OVCAR3 cells after 48 h of exposure to BSO (magnification 200×). **b** Cell death evaluation by FACS, annexin V, and PI staining. OVCAR3 and ES2 cells were treated with different combinations of carboplatin and H_2O_2 (positive control), for 16 h. Whenever applied, cells were either previously exposed to BSO (20 mM) for 48 h or in concomitance with carboplatin (25 μg/mL) and/ or H_2O_2 (98 μM). *Error bars* represent standard deviation; statistical significance *$p<0.05$, **$p<0.01$, ***$p<0.001$
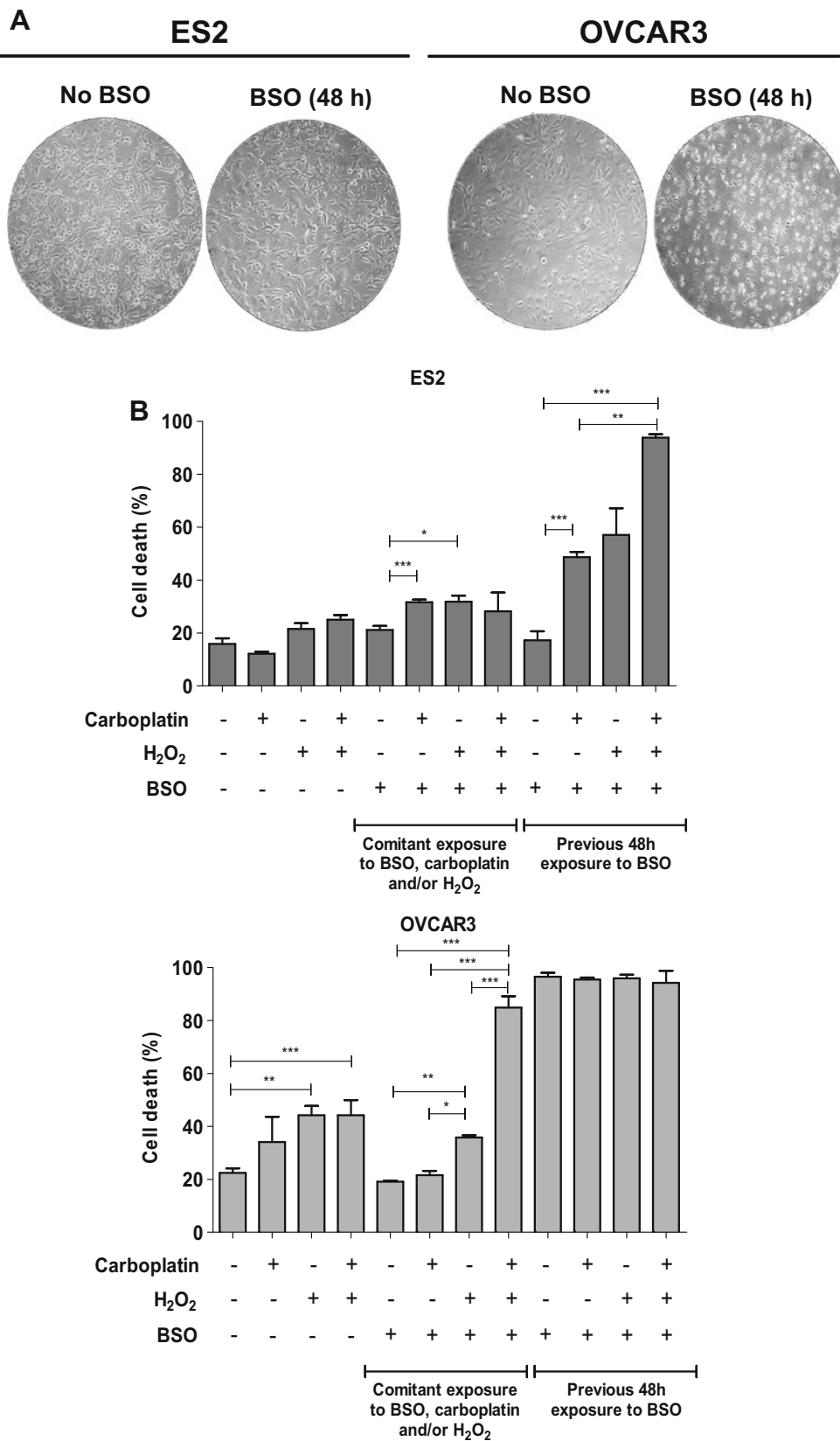
express low levels of GCLC even in L-glutamine plus L-cysteine supplemented medium (Fig. 7b). As expected,

HNF1β knockdown did not affect the expression in GCLM (Fig. 7b).
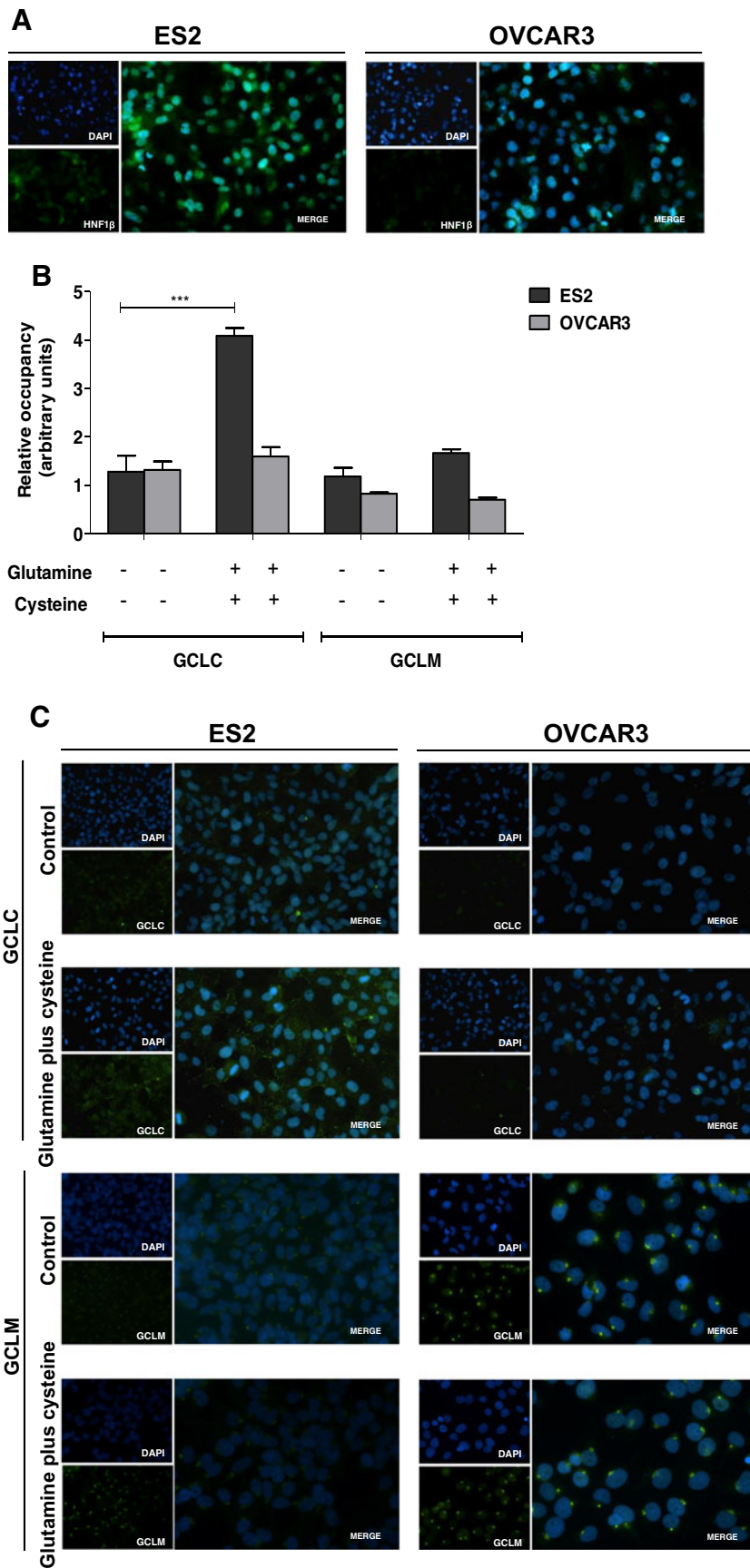
◀ **Fig. 6** HNF1β regulates γ-glutamylcysteine ligase catalytic subunit (GCLC) but not modifier subunit (GCLM) expression in ES2. **a** Expression of HNF1β in ES2 and OVCAR3 cells by immunofluorescence (magnification 200×). Nuclei DAPI (*blue*), HNF1β FITC (*green*). **b** Relative occupancy of HNF1β at *GCLC* and *GCLM* promoter determined by ChIP assay. Cells were cultured for 48 h in the presence and absence of L-glutamine plus L-cysteine. **c** Expression of GCLC and GCLM in ES2 and OVCAR3 cells by immunofluorescense (magnification 200×). Nuclei DAPI (*blue*), GCLC, and GCLM FITC (*green*). *Error bars* represent standard deviation; statistical significance ***p<0.001

Interestingly, ES2 cells HNF1β knockdown revealed to be more sensitive to BSO and carboplatin-induced death (Fig. 7c). This experimental approach revealed that HNF1β is responsible for the regulation of GSH production, underlying carboplatin resistance.

In vivo model validates BSO as a chemo-adjuvant (sensitizer) for carboplatin therapy in OCCC

The in vivo BALB-c\SCID model of OCCC, in order to validate BSO as an adjuvant drug for carboplatin therapy, showed that both subcutaneous tumors and peritoneal spread visually decreased in mice treated with BSO 24 h prior to carboplatin administration, as compared to control mice and mice treated separately with BSO or carboplatin (Fig. 8a, b). Nevertheless, mice treated in separate with BSO and carboplatin showed less peritoneal tumors than control mice, despite no differences were observed in the subcutaneous tumors (Fig. 8a). Accordingly, GSH measurements, made in tumor extracts, showed the highest levels in tumors from control mice and the lowest in mice treated with BSO plus carboplatin. While mice treated exclusively with BSO or carboplatin showed intermediate levels of GSH (Fig. 8c).

Discussion

In the present study, we aimed to clarify if HNF1β is responsible for the chemoresistance to platinum-based chemotherapy exhibited by OCCC [3, 9–11]. Contrary to other histological types in which chemoresistance is an acquired phenomenon, in OCCC extraovarian disease, which cannot be cured by surgery, chemoresistance is an intrinsic feature. Hence, OCCC recurrent disease after surgery and advanced disease at diagnosis do not respond to platinum-based conventional therapy.

For this purpose, two different histological in vitro models from EOC were studied, representing a highly chemoresistant type (OCCC) and the most frequent (OSC) histological type, which is more sensitive to chemotherapy [3, 9–11]. Since metabolic alterations are evident in OCCC, due to HNF1β de novo expression, we studied glutaminolysis in these
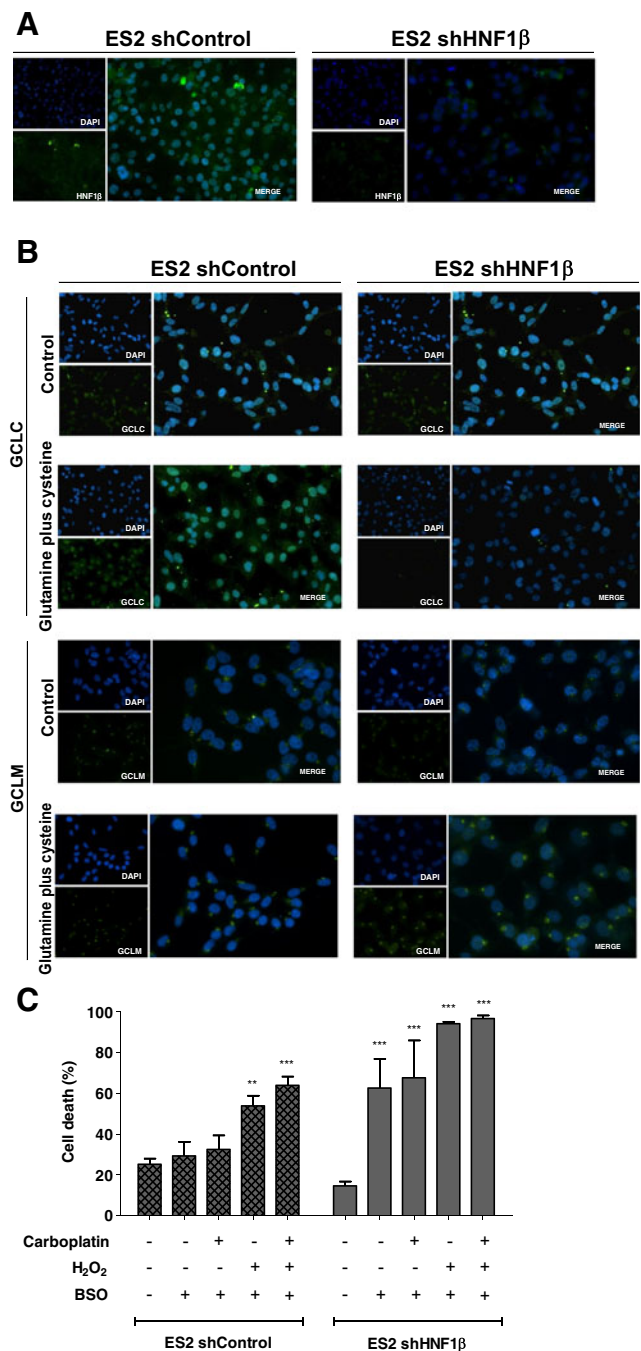
Fig. 7 HNF1β knock down in ES2 cell line confirms its role in γ-glutamylcysteine ligase (GCLC) expression. HNF1β knocked down ES2 cell line are more sensitive to carboplatin. **a** Expression of HNF1β in shControl and shHNF1β ES2 cells by immunofluorescence (magnification 200×). Nuclei DAPI (*blue*), HNF1β FITC (*green*). **b** Expression of GCLC and GCLM in shControl and shHNF1β ES2 cells by immunofluorescense (magnification 200×). Nuclei DAPI (*blue*), GCL, and GCLM FITC (*green*). **c** Cell death evaluation by FACS, annexin V, and PI staining. shControl and shHNF1β ES2 cells were previously exposed to BSO (20 mM) for 48 h and after that treated with different combinations of carboplatin (25 μg/mL) and H₂O₂ (98 μM, positive control) for 16 h. *Error bars* represent standard deviation; statistical significance **p<0.01, ***p<0.001
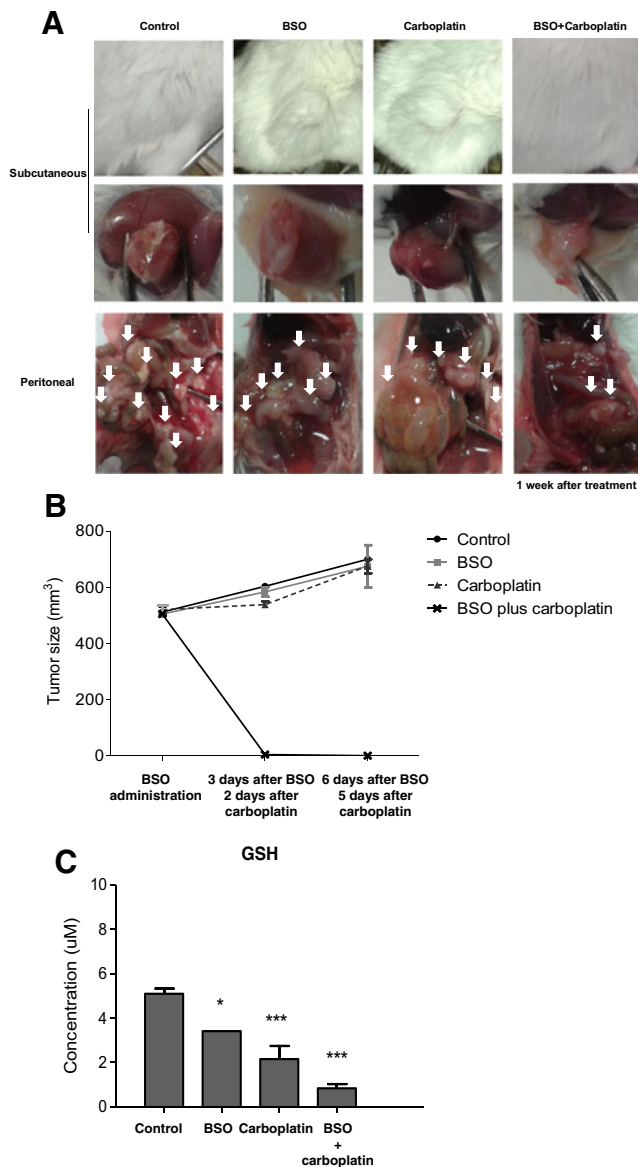
Fig. 8 In vivo model of OCCC confirms that abrogation of GSH production by BSO increases sensitivity to carboplatin. Tumor size and GSH levels dramatically decreased in mice treated with both BSO and carboplatin. **a** Subcutaneous tumors and peritoneal spread (*white arrows*) in mice control and treated with BSO, carboplatin, and BSO plus carboplatin. BSO was administrated 24 h before carboplatin. **b** The volume of subcutaneous tumors (mm³) in mice before and along treatment. **c** GSH levels quantification by HPLC in tumor extracts. *Error bars* represent standard deviation; statistical significance *p<0.05, **p<0.01, ***p<0.001

tumors. It is known that L-glutamine is a frequently used carbon, nitrogen, and energy source for cancer cells in detriment of glucose [33, 34] and glutamine importantly originates GSH precursor amino acids.

The metabolic profile obtained by NMR showed that glutaminolysis is active in both OCCC and OSC cells. However, cell lines presented different metabolic profiles, since resulting products of glutaminolysis were shown to divert into different biological purposes. In ES2 (OCCC), the detected L-glutamine-derived metabolites are mainly amino acids and GSH, and in OVCAR3 (OSC), besides amino acids and GSH, TCA cycle intermediates and metabolites from phosphatidylcholine degradation are also detected (Fig. 2a). Interestingly, phosphatidylcholine is the main phospholipid component in eukaryotic membranes and high rates of phosphatidylcholine degradation has been previously described in EOC [35] and known to be related to increased proliferation rates [19, 36]. By cell cycle analysis, comparing both cell lines, we demonstrate that OVCAR3 proliferates at a higher rate than ES2 (Fig. 2b), which fits with its metabolic profile.

Additionally, comparing to the respective control conditions, both cell lines showed a higher rate of proliferation when cultured in L-glutamine-supplemented media. This fact corroborates that L-glutamine is a crucial metabolic element [19, 28, 37] and steams for the putative inhibition of glutaminolytic enzymes as a good strategy to disturb cancer cells proliferation [29].

GSH was detected predominantly intracellular in both cell lines, as shown by NMR (Fig. 2a) and HPLC (Figs. 2 and 3). As expected, supplementation with L-glutamine plus L-cysteine displayed higher GSH levels, since both L-glutamate and L-glycine (derived from glutaminolysis, as seen by NMR) and L-cysteine are the components of GSH. Comparing the two cell lines, GSH levels were higher in ES2 (OCCC) than OVCAR3, which is in agreement with NMR results, showing that ES2 cells use almost exclusively L-glutamine to produce amino acids and GSH (Figs. 2a and 3d). The higher levels of L-cysteine uptake in ES2 cells, comparing to OVCAR3, also contribute to the higher GSH levels (Fig. 4a).

Interestingly, cell death analysis showed that ES2 is 3-fold more resistant to carboplatin than OVCAR3 (Fig. 5b), as it is described for OCCC. This fact corroborates the link between high levels of GSH and increased chemoresistance [24, 38, 39].

Looking in depth, four possible scenarios can underlie the aminothiol-mediated cell resistance to carboplatin: (1) an increased rate of GSH synthesis; (2) a decreased rate of GSH degradation; (3) an increase in extracellular levels of thiols, sequestering carboplatin and avoiding its influx; and (4) an increase in intracellular levels of thiols, scavenging carboplatin and ROS.

As seen in our experiments, ES2 cell line produces higher levels of GSH compared with OVCAR3. Upon exposure to carboplatin and comparing within conditions in the absence of carboplatin in each cell line, GSH levels increase both in ES2 and OVCAR3, except in ES2 L-glutamine plus L-cysteine condition which decreases GSH levels, though it remains high (Fig. 3d). As carboplatin is a platinum-based anti-cancer drug, capable of promoting cell cycle arrest and apoptosis, by inducing the production of ROS [40, 41], this molecular

adjustment might be explained by the need of GSH as an antioxidant. Under carboplatin exposure, in ES2, GSH was still found, mainly inside cells, and remained higher than in OVCAR3 (Fig. 3d). Regarding, the carboplatin-related increase in extracellular GSH levels (Fig. 4d) in OVCAR3, it can be explained by the high percentage of cell death, due to the rupture of cell membrane and the release of GSH to the extracellular medium (Fig. 5b).

The difference in GSH levels between ES2 and OVCAR3 cell lines partially relies on HNF1β upregulation, which is a distinctive feature of OCCC cells [34, 42]. Indeed, we confirmed HNF1β was expressed in ES2 cells and not in OVCAR3 (Fig. 6a), and interestingly, by ChIP, we proved that HNF1β binds more to GCLC gene promoter, corresponding to an increased GCLC expression in ES2 cells cultured in L-glutamine plus L-cysteine-supplemented medium, as compared to control conditions as well as to OVCAR3 (Fig. 6b, c). We proved the role of HNF1β in CGLC regulation, by knocking down HNF1β, and this promoted a decrease in GCLC expression in ES2 (Fig. 6a, b). These data show that HNF1β is implicated in GSH synthesis, emerging then as a putative underlying agent in intrinsic OCCC chemoresistance. Although the regulation of CGLC and GCLM expression by the oxidative stress is described as being mediated by Nrf2 transcription factor, in the present OCCC cancer model HNF1β definitely has a role [43, 44]. Interestingly, GCLM expression is not regulated by HNF1β in ES2 being also its expression independent of L-glutamine availability (Fig. 7b). In addition, the fact that OVCAR3 express high levels of GCLM may shed a light to a molecular mechanism underlying the acquisition of chemoresistance in OSC.

Regarding GSH degradation, CYS-GLY is a metabolite resultant from GSH degradation by γ-glutamyl transferase (GGT), a cell membrane enzyme. Curiously, in ovarian carcinomas, GGT expression has been already reported as part of a "cell resistance phenotype" [45]. A pattern of CYS-GLY similar to GSH was observed in both cell lines, though upon exposure to carboplatin, a decrease in intracellular amounts (Fig. 3c) was observed whereas extracellular levels remained unaltered (Fig. 4c). This observation indicates a decreased GSH catabolism that might be related to the flow of GSH for cell protection. Of notice, CYS-GLY extracellular levels in ES2 were higher than in OVCAR3 (Fig. 4c), which by itself can contribute for chemoresistance, as depicted further. In addition, the *ratio* GSH/CYS-GLY in ES2 is inverted between intracellular (GSH/CYS-GLY = 10) and extracellular (GSH/CYS-GLY = 0.5-fold) media, pointing out a high and continuous rate of GSH production.

It is known that in cells, a large part of carboplatin will react promptly with the highly nucleophilic sulfur-containing molecules; thus, a higher intracellular thiol pool will be able to capture carboplatin, avoiding the arrival to its target, the DNA, contributing to a lower cell effect (Fig. 9). As so, CYS, HCYS,

CYS-GLY, and GSH intra- and extracellular dynamics can act as cell-protecting mechanisms, explaining the two last mechanisms proposed for GSH-related chemoresistance [46]. The decrease of intracellular CYS-GLY, comparing with the levels observed in the absence of carboplatin, is likely associated to its export to extracellular compartment in order to putatively form adducts with carboplatin, preventing its detection by HPLC (Fig. 4c). Also, as GSH is used for carboplatin and ROS scavenging, it is spared and the catabolism decreased. This fact also explains the decreased, although still high, GSH levels in ES2 cultured in L-glutamine plus L-cysteine upon carboplatin exposure (Fig. 3d), since GSH involved in GSH-carboplatin adducts are not detected by the used HPLC method. Again, the maintenance of very high amounts of GSH in ES2 claims the existence of a continuous internal loop of GSH production, certainly mediated by HNF1β.

The decrease in HCYS due to carboplatin exposure (Figs. 3b and 4b) can be related to its role as a scavenger or to as precursor in the CYS synthesis. In cells, CYS can act as a scavenger or be used in GSH synthesis. This is supported by our data from cells cultured with L-cysteine (CYS), in which a higher influx of CYS is observed. However, this influx did not induce an increase of GSH synthesis, meaning that CYS, in this cancer model, can work by itself as a scavenger of carboplatin and ROS (Figs. 2a and 3a).

These observations led us to consider GSH as a putative underlying agent in OCCC platinum-drugs chemoresistance because the efficiency of platinum-based chemotherapeutic agents depends on the drug quantity that reaches the DNA and on the alteration of redox state through ROS generation. Indeed, GSH system has been already proposed as a possible target for medical intervention against cancer progression and chemoresistance [18, 23, 24].

Taken together, the increased synthesis of GSH seems to be a very important mechanism working on OCCC cells resistant to carboplatin, being supported by the evaluation of cell death upon the inhibition of GSH synthesis using BSO (Fig. 5). BSO is a chemical compound that inhibits GCL enzyme. Treatment with carboplatin and/or H_2O_2 resulted in an increase in OVCAR3 cell death, in comparison with ES2, for which the use of these oxidative stress inducers did not affect cell viability. The previous sensitization of cells by BSO induced a significant increase in ES2 cell death, as well as for OVCAR3, in which it was even more remarkable (Fig. 5b). Apoptosis and necrosis contribution for overall cell death was equivalent for both cell lines (data not shown).

As mentioned, carboplatin resistance is an intrinsic feature of OCCC, proved by the clinical observation that extraovarian disease (recurrence after surgery or advanced disease at diagnosis) do not respond to carboplatin therapy [3, 9–11]. Seeking the role of HNF1β in OCCC chemoresistance, we propose that the maintenance of an internal loop driven by HNF1β and GCLC sustains high GSH levels in OCCC cell
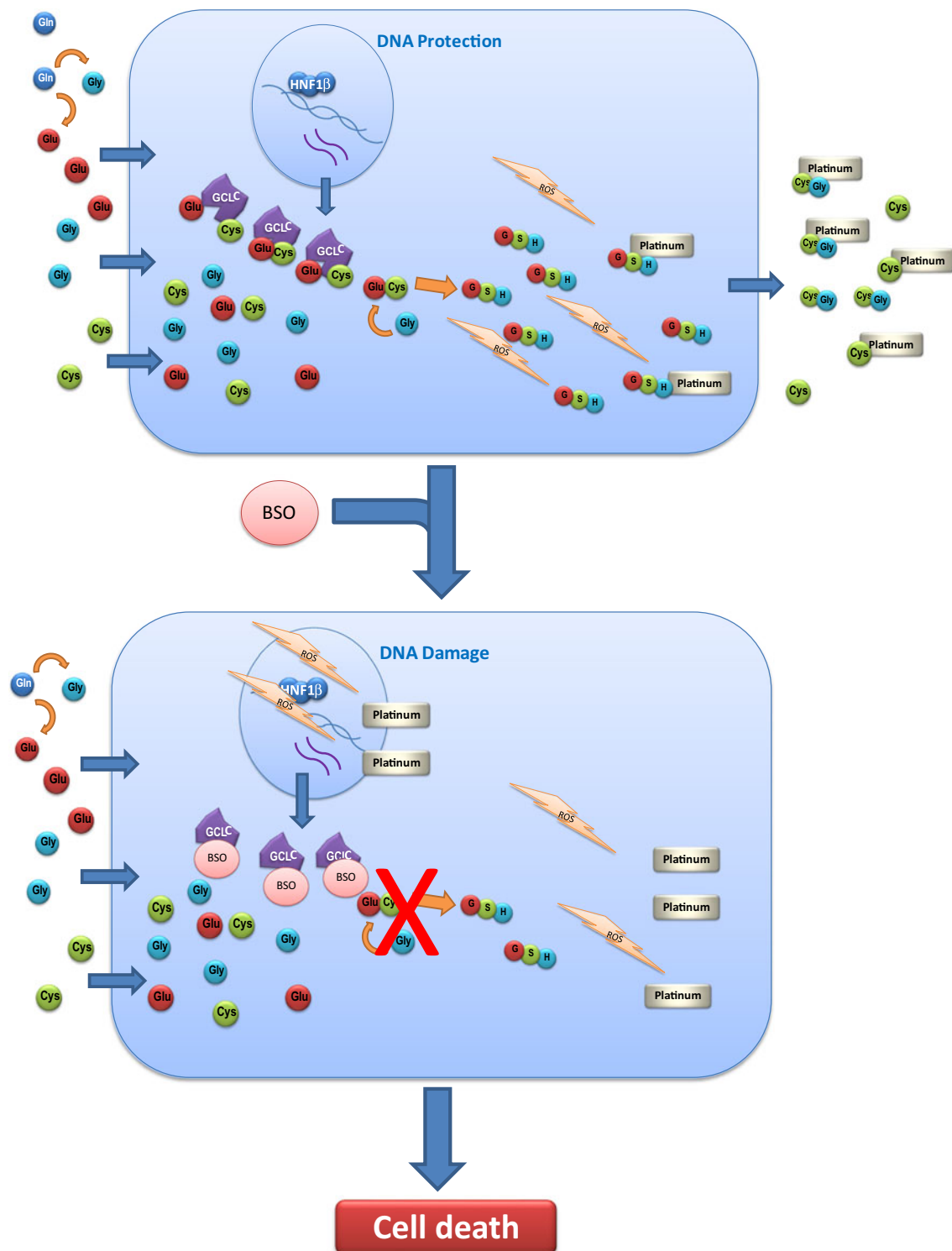
Fig. 9 Scheme of a therapeutic strategy to overcome the HNF1β-dependent molecular mechanism underlying thiol-mediated chemoresistance in OCCC. The exposure of cells to GCL inhibitors, namely buthionine sulphoxamine (BSO), prior to the use of platinum based therapy will abrogate GSH synthesis and sensitize cells to drugs and trigger cell death

line (ES2), protecting these cells from death by DNA-damaging and ROS-generating agents. Moreover, we also propose a mechanism of continuous restoration of GCLC levels that maintains thiols capacity of carboplatin blockage

(Fig. 9). To understand the acquired resistance of OSC to chemotherapy, it would be interesting to evaluate the levels of GCLM in OVCAR3 upon long-term carboplatin exposure. However, this issue would not be addressed in this paper.

As mentioned above, the fact that ES2 culture conditions showing the highest levels of GSH, HNF1β, and GCL expression as well as the binding of HNF1β to the promoter of *GCLC* gene (Fig. 6) strengthen our hypothesis. The knockdown of HNF1β and the consequent decreased GCLC expression in ES2 (Fig. 7) were the final confirmation that this transcription factor de novo expressed in OCCC regulates GCLC expression and consequently GSH production. Finally, it was observed that ES2 knocked down cells are more sensitive to carboplatin (Fig. 7c).

The corolarium of this study was the in vivo model (Fig. 8a, b), showing a dramatic decrease in tumor burden, both in subcutaneous and peritoneal tumors, due to the sequentially combined administration of BSO and carboplatin. The effect of BSO in GSH production in tumor cells was evident in the measurement of GSH levels, showing the lowest levels in tumors from mice treated with BSO plus carboplatin (Fig. 8c).

About 20 years ago, some studies addressing BSO as an alternative to abrogate GSH in cancer cells were published [47–49]; however, no worth cancer therapeutic alternative was registered. Probably, this is because the systemic GSH abrogation will be a devastating phenomenon with severe adverse effects in a human body. Nevertheless, we believe that BSO is a good drug to sensitize OCCC tumors to conventional chemotherapy as seen in our presented models. Probably, the use of targeted nanoparticles will help to bypass this critical step in the delivery of BSO to cancer cells. In addition, we think that peritoneal infusion will probably be a more suitable administration route since nanoparticles have a low absorption rate by peritoneum.

Summing up, our study discloses HNF1β as the mediator of the mechanism underlying intrinsic OCCC chemoresistance and sheds a light in a re-explored cancer adjuvant therapeutic approach in order to overcome the lack of efficient therapy for OCCC.

References

1. Feeley KM, Wells M. Precursor lesions of ovarian epithelial malignancy. Histopathology. 2001;38:87–95. Available from: http://www.ncbi.nlm.nih.gov/pubmed/11207821.

2. Siegel R, Naishadham D, Jemal A. Cancer Statistics, 2012. Cancer J Clin. 2012;62:10–29.

3. Sugiyama T, Kamura T, Kigawa J, Terakawa N, Kikuchi Y, Kita T, et al. Clinical characteristics of clear cell carcinoma of the ovary: a distinct histologic type with poor prognosis and resistance to platinum-based chemotherapy. Cancer. 2000;88:2584–9. Available from: http://www.ncbi.nlm.nih.gov/pubmed/10861437.

4. Verhaak RGW, Tamayo P, Yang J, Hubbard D, Zhang H, Creighton CJ, et al. Prognostically relevant gene signatures of high-grade serous ovarian carcinoma. J Clin Invest. 2013;123:517–25.

5. Del Carmen MG, Birrer M, Schorge JO. Clear cell carcinoma of the ovary: a review of the literature. Gynecologic oncology [Internet]. Elsevier Inc.; 2012 [cited 2015 Jan 29];126:481–90. Available from: http://www.ncbi.nlm.nih.gov/pubmed/22525820

6. Gates C, Rice VM. Epithelial ovarian cancer: an overview. World J Transl Med. 2014;3:10–29.

7. Mabuchi S, Kawase C, Altomare DA, Morishige K, Sawada K, Hayashi M, et al. mTOR is a promising therapeutic target both in cisplatin-sensitive and cisplatin-resistant clear cell carcinoma of the ovary. Clin Cancer Res Off J Am Assoc Cancer Res. 2009;15:5404–13. Available from: http://www.pubmedcentral.nih.gov/articlerender.fcgi?artid=2743856&tool=pmcentrez&rendertype=abstract.

8. Shen H, Fridley BL, Song H, Lawrenson K, Cunningham JM. Epigenetic analysis leads to identification of HNF1B as a subtype-specific susceptibility gene for ovarian cancer. Nat Commun. 2013;4.

9. Lee Y-Y, Kim T-J, Kim M-J, Kim H-J, Song T, Kim MK, et al. Prognosis of ovarian clear cell carcinoma compared to other histological subtypes: a meta-analysis. Gynecologic oncology [Internet]. Elsevier Inc.; 2011 [cited 2015 Feb 27];122:541–7. Available from: http://www.ncbi.nlm.nih.gov/pubmed/21640372

10. Pather S, Quinn MA. Clear-cell cancer of the ovary—is it chemosensitive ? Int J Gynecol Cancer. 2005;15:432–7.

11. Anglesio MS, Carey MS, Köbel M, Mackay H, Huntsman DG. Clear cell carcinoma of the ovary: a report from the first Ovarian Clear Cell Symposium, June 24th, 2010. Gynecologic oncology [Internet]. Elsevier Inc.; 2011 [cited 2013 Sep 22];121:407–15. Available from: http://www.ncbi.nlm.nih.gov/pubmed/21276610

12. Konstantinopoulos PA, Matulonis UA. Current status and evolution of preclinical drug development models of epithelial ovarian cancer. Frontiers in Oncol. 2013;3:296. Available from: http://www.pubmedcentral.nih.gov/articlerender.fcgi?artid=3858677&tool=pmcentrez&rendertype=abstract.

13. Verschoor ML, Singh G. Ets-1 regulates intracellular glutathione levels: key target for resistant ovarian cancer. Mol Cancer. 2013;12:138. Available from: http://www.pubmedcentral.nih.gov/articlerender.fcgi?artid=3842663&tool=pmcentrez&rendertype=abstract.

14. Chaney SG, Campbell SL, Temple B, Bassett E, Wu Y, Faldu M. Protein interactions with platinum-DNA adducts: from structure to function. J Inorg Biochem. 2004;98:1551–9. Available from: http://www.ncbi.nlm.nih.gov/pubmed/15458816.

15. Goodisman J, Hagrman D, Tacka KA, Souid A-K. Analysis of cytotoxicities of platinum compounds. Cancer Chemother Pharmacol. 2006;57:257–67. Available from: http://www.ncbi.nlm.nih.gov/pubmed/16028101.

16. Unger FT, Klasen HA, Tchartchian G, de Wilde RL, Witte I. DNA damage induced by cis- and carboplatin as indicator for in vitro sensitivity of ovarian carcinoma cells. BMC Cancer. 2009;9:359. Available from: http://www.pubmedcentral.nih.gov/articlerender.fcgi?artid=2768745&tool=pmcentrez&rendertype=abstract.

17. Wang D, Lippard SJ. Cellular processing of platinum anticancer drugs. Nat Rev Drug Discov. 2005;4:307–20.

18. Dhivya H. Glutathione—a master antioxidant and an immune system modulator. 2012;1:13–5.

19. Matés JM, Segura JA, Martín-Rufián M, Campos-Sandoval JA, Alonso FJ, Márquez J. Glutaminase isoenzymes as key regulators in metabolic and oxidative stress against cancer. Current Mol Med. 2013;13:514–34. Available from: http://www.ncbi.nlm.nih.gov/pubmed/22934847.

20. Yang Y, Dieter MZ, Chen Y, Shertzer HG, Nebert DW, Dalton TP. Initial characterization of the glutamate-cysteine ligase modifier subunit Gclm(-/-) knockout mouse. Novel model system for a severely compromised oxidative stress response. J Biol Chem. 2002;277:49446–52. Available from: http://www.ncbi.nlm.nih.gov/pubmed/12384496.

21. Franklin CC, Backosa DS, Moharb I, White CC, Formanc JH, et al. Structure, function, and post-translational regulation of the catalytic and modifier subunits of glutamate cysteine ligase. Mol Aspects Med. 2010;30:86–98.

22. Kelland LR. Preclinical perspectives on platinum resistance. Drugs. 2000;59:1–8.

23. Estrela JM, Ortega A, Obrador E. Glutathione in cancer biology and therapy. Crit Rev Clin Lab Sci. 2006;43:143–81. Available from: http://www.ncbi.nlm.nih.gov/pubmed/16517421.

24. Traverso N, Ricciarelli R, Nitti M, Marengo B, Furfaro AL, Pronzato MA, et al. Role of glutathione in cancer progression and chemoresistance. Oxidative medicine and cellular longevity [Internet]. 2013;2013:972913. Available from: http://www.pubmedcentral.nih.gov/articlerender.fcgi?artid=3673338&tool=pmcentrez&rendertype=abstract

25. Corti A, Franzini M, Paolicchi A, Pompella A. Gamma-glutamyltransferase of cancer cells at the crossroads of tumor progression, drug resistance and drug targeting. Anticancer Res. 2010;30:1169–81. Available from: http://www.ncbi.nlm.nih.gov/pubmed/20530424/RefSource>.

26. Serpa J, Dias S. Metabolic cues from the microenvironment act as a major selective factor for cancer progression and metastases formation. Cell Cycle. 2011;10:180–1. Available from: http://www.landesbioscience.com/journals/cc/article/14476/.

27. Hanahan D, Weinberg RA. Hallmarks of cancer: the next generation. Cell Elsevier Inc. 2011;144:646–74. Available from: http://www.ncbi.nlm.nih.gov/pubmed/21376230.

28. Dang CV. Glutaminolysis: supplying carbon or nitrogen, or both for cancer cells? Cell Cycle. 2010;9:3884–6. Available from: http://www.landesbioscience.com/journals/cc/article/13302/.

29. Reynolds MR, Lane a N, Robertson B, Kemp S, Liu Y, Hill BG, et al. Control of glutamine metabolism by the tumor suppressor Rb. Oncogene [Internet]. Nature Publishing Group; 2013 [cited 2013 Jul 6];1–11. Available from: http://www.ncbi.nlm.nih.gov/pubmed/23353822

30. Fath MA, Ahmad IM, Smith CJ, Spence J, Spitz DR. Enhancement of carboplatin-mediated lung cancer cell killing by simultaneous disruption of glutathione and thioredoxin metabolism. Clin Cancer Res Off J Am Assoc Cancer Res. 2011;17:6206–17. Available from: http://www.pubmedcentral.nih.gov/articlerender.fcgi?artid=3186854&tool=pmcentrez&rendertype=abstract.

31. Watanabe T, Sagisaka H, Arakawa S, Shibaya Y, Watanabe M. A novel model of continuous depletion of glutathione in mice with L-butathione (S, R)-sulfoximine. J Toxicol Sci Toxicol Sci. 2003;28:455–69.

32. Meijer C, Mulder NH, Timmer-bosscha H. Relationship of cellular glutathione to the cytotoxicity and resistance of seven platinum compounds[1]. Cancer Res. 1992;52:6885–9.

33. Daye D, Wellen KE. Metabolic reprogramming in cancer: unraveling the role of glutamine in tumorigenesis. Seminars in cell & developmental biology. Elsevier Ltd; 2012;23:362–9. Available from: http://www.pubmedcentral.nih.gov/articlerender.fcgi?artid=3186854&tool=pmcentrez&rendertype=abstract.

34. Shen H, Fridley BL, Song H, Lawrenson K, Cunningham JM, Ramus SJ, et al. Epigenetic analysis leads to identification of HNF1B as a subtype-specific susceptibility gene for ovarian cancer. Nat Commun. 2013;4:1628. Available from: http://www.pubmedcentral.nih.gov/articlerender.fcgi?artid=3848248&tool=pmcentrez&rendertype=abstract.

35. Iorio E, Mezzanzanica D, Alberti P, Spadaro F, Ramoni C, D'Ascenzo S, et al. Alterations of choline phospholipid metabolism in ovarian tumor progression. Cancer Res. 2005;65:9369–76. Available from: http://www.ncbi.nlm.nih.gov/pubmed/16230400.

36. Ridgway ND. The role of phosphatidylcholine and choline metabolites to cell proliferation and survival. Crit Rev Biochem Mol Biol. 2013;48:20–38. Available from: http://www.ncbi.nlm.nih.gov/pubmed/16230400.

37. Israël M, Schwartz L. The metabolic advantage of tumor cells. Molecular cancer [Internet]. BioMed Central Ltd; 2011 [cited 2013 May 31];10:70. Available from: http://www.pubmedcentral.nih.gov/articlerender.fcgi?artid=3118193&tool=pmcentrez&rendertype=abstract

38. Blair SL, Heerdt P, Sachar S, Aboihoda A, Hochwald S, Cheng H, et al. Glutathione metabolism in patients with non-small cell lung cancers. Cancer Res. 1997;152:152–6.

39. Wu JH, Batist G. Glutathione and glutathione analogues; therapeutic potentials. Biochimica et biophysica acta [Internet]. Elsevier B.V.; 2013 [cited 2015 Feb 26];1830:3350–3. Available from: http://www.ncbi.nlm.nih.gov/pubmed/23201199

40. Husain K, Whitworth C, Somani SM, Rybak LP. Carboplatin-induced oxidative stress in rat cochlea. Hear Res. 2001;159:14–22. Available from: http://www.ncbi.nlm.nih.gov/pubmed/11520631.

41. Quintana E, Pertusa J, González R, Renau-Piqueras J. Carboplatin treatment induces dose-dependent increases in the frequency of micronuclei in Ehrlich ascites tumor cells. Mutat Res. 1994;322:55–60. Available from: http://www.ncbi.nlm.nih.gov/pubmed/7517504.

42. Tsuchiya A, Sakamoto M, Yasuda J, Chuma M, Ohta T, Ohki M, et al. Expression profiling in ovarian clear cell carcinoma. Am J Pathol Am Soc Investig Pathol. 2003;163:2503–12. Available from: http://linkinghub.elsevier.com/retrieve/pii/S000294401063605X.

43. Lee J-M, Calkins MJ, Chan K, Kan YW, Johnson JA. Identification of the NF-E2-related factor-2-dependent genes conferring protection against oxidative stress in primary cortical astrocytes using oligonucleotide microarray analysis. J Biol Chem. 2003;278:12029–38.

44. Singhal SS, Yadav S, Roth C, Singhal J. RLIP76: a novel glutathione-conjugate and multi-drug transporter. Biochem Pharmacol. 2009;77:761–9. Available from: http://www.pubmedcentral.nih.gov/articlerender.fcgi?artid=2664079&tool=pmcentrez&rendertype=abstract.

45. Pompella A, De Tata V, Paolicchi A, Zunino F. Expression of gamma-glutamyltransferase in cancer cells and its significance in drug resistance. Biochem Pharmacol. 2006;71:231–8. Available from: http://www.ncbi.nlm.nih.gov/pubmed/16303117.

46. Jerremalm E, Wallin I, Yachnin J, Ehrsson H. Oxaliplatin degradation in the presence of important biological sulphur-containing compounds and plasma ultrafiltrate. European J Pharm Sci Off J European Federation for Pharm Sci. 2006;28:278–83.

47. Green JA, Vistica DT, Young RC, Hamilton TC, Rogan AM, Ozols RF. Potentiation of melphalan cytotoxicity in human ovarian cancer cell lines by glutathione depletion. Cancer Res. 1984;44:5427–31.

48. Russo A, Degraff W, Friedman N, Mitchell JB. Selective modulation of glutathione levels in human normal versus tumor cells and subsequent differential response to chemotherapy drugs. Cancer Res. 1986;46:2845–8.

49. Fojo A, Hamilton T, Young R, Ozols R. Multidrug resistance in ovarian cancer. Cancer. 1987;60:2075–80.

50. Nolin TD, McMenamin ME, Himmelfarb J. Simultaneous de-
     termination of total homocysteine, cysteine, cysteinylglycine,
     and glutathione in human plasma by high-performance liquid
     chromatography: application to studies of oxidative stress. J
     Chromatogr B Analyt Technol Biomed Life Sci. 2007;852:
     554–61. Available from: http://www.pubmedcentral.nih.gov/
     articlerender.fcgi?artid = 1959569&tool=pmcentrez&rendertype=
     abstract.